Nonlinear ultrasound fields simulation of harmonics from exponential and bessel beams sources

Hicham Jakjoud[a], Ahmed Chitnalah[a], Noureddine Aouzale[a] and Djilali Kourtiche[b]

[a]Lab. Electrical Systems and Telecommunications, Faculté des Sciences et Techniques Gueliz B.P. 549, 40000 Marrakech, Morocco

[b]Lab. d'Instrumentation, Electronique de Nancy, UHP Nancy I, BP 239, 54506 Vandœuvre, 54506 Nancy, France

hicham.jakjoud@gmail.com

It's well known that the harmonic imaging quality can be improved by using sources that radiate narrower and attenuated sidelobes beams. Hence we try to enhance the harmonics' cartography by studying different source's power distributions. We developed a numerical code, using the spectral method, in order to resolve the parabolic wave equation. The numerical results were compared to the results given by Bergen code in order to validate our algorithm. Two source's power distributions (exponential and Bessel beams) were studied and compared to the uniform case.

The use of exponential source leaded to harmonics diagrams without sidelobes neither nearfield oscillations. But the beam width was increasing with propagation.

The Bessel source presents a limited diffraction beam. The beam width is almost constant throughout the nearfield and the transition zone. The sidelobes had a weak level in the fundamental curves and they don't appear in the second harmonic ones.

1   Introduction

The quality of images provided by ultrasound imaging systems is closely related to the radiation pattern of the source. It's important to get the best resolution and the highest contrast. One can use focused source to improve lateral and axial resolution [1,2]. Recently harmonic imaging [3,4] was developed and gets better images quality. This is due to the fact that the harmonic beams are narrower and shows attenuated sidelobes [4].

However, image quality in terms of resolution and contrast still need to be enhanced. What leads researchers to study "adopized sources". The adopization allows getting an arbitrary power distribution on the surface of the transducer. Hence exponential, cosine and Bessel shapes have been studied. The exponential sources present beams with no sidelobes. Cosine sources present narrower beams. Whereas the Bessel beams show a limited diffraction character.

We studied the exponential aperture [5] and compared the obtained results to the uniform and cosine ones. The exponential beams showed more interesting characteristics for imaging applications than the two others sources. Recently, we studied cosine based apertures [6] which are written as $\cos^{1/q}(\xi)$ with q is an integer and ξ is the transverse variable. The results were compared to Gaussian beams. We, hence, noted that the value of q can improve the cosine aperture's features for imaging systems. Ding and Lu [8] presented the expressions of the fundamental and the second harmonic for a Bessel source. They showed that the second harmonic's width is a half of the fundamental one.

In the present study we compared the harmonic patterns of an exponential and a Bessel shaped sources. We developed a resolution code [6,9] for the Khokhlov-Zabolotskaya-Kuznetsov equation (KZK). The algorithm is based on the spectral method and allowing computing for several source conditions. Our source is a $a = 0.5cm$ radius piezoelectric disc transmitting at the central frequency of $f_0 = 2.2MHz$ and with a power density of 1W/cm² in distilled water.

2   Theoretical basis

The KZK model [10,11] model is commonly used to describe non linear ultrasound propagation in a thermoviscous fluid. Many studies [12-16] dealt with integration of the KZK equation using spectral method. The most famous algorithm is the Bergen code presented by Aanonsen et al. [12]. Hamilton et al. [14] transformed the KZK equation to the transformed beam equation (TBE) in order to accelerate the integration in the farfield zone. The validity of the KZK model and the Bergen code has been proved by the experimental studies.

Let's consider the propagation of a wave through the z axis. From a circular source positioned at z=0. The parabolic equation is written in cylindrical coordinates [10,11]:

$$\frac{\partial^2 p}{\partial\sigma\partial\tau} = \frac{2z_0}{c_0}\nabla_\perp^2 p + \frac{2Dz_0}{c_0^3}\frac{\partial^3 p}{\partial\tau^3} + \frac{2\beta z_0}{\rho_0 c_0^3}\frac{\partial^2 p^2}{\partial\tau^2} \quad (1)$$

Where $\sigma = z/z_0$, $\xi = r/a$ and $z_0 = k_0 a^2/2$ is the Rayleigh distance, $k_0 = f_0/c_0$ is the wave number. D is the sound diffusivity, it accounts for viscosity, thermal conduction and relaxation. $\beta = 1 + B/2A$ is the parameter of the ultrasonic nonlinearity, c_0 is the small signal speed, ρ_0 is the medium density at rest, and $\tau = t - z/c_0$ is the retarded time.

$\nabla_\perp^2 = \frac{1}{a^2}\left(\frac{1}{\xi}\frac{\partial}{\partial\xi} + \frac{\partial^2}{\partial\xi^2}\right)$ is the transverse Laplacian operator.

The field pressure is written in terms of Fourier series as bellow:

$$p(\sigma,\xi) = \sum_{-\infty}^{\infty} p_n(\sigma,\xi)\, e^{2\pi i n f_0 \tau} \quad (2)$$

We use the following discretization:

$$\sigma = i\Delta\sigma \qquad i = 1, 2, ..., I$$
$$\xi = j\Delta\xi \qquad j = 1, 2, ..., J \quad (3)$$
$$p_n(\xi,\sigma) = p_n^{i,j}$$

Where I and J are the maxima values of i and j respectively defining the maxima ranges of σ and ξ ($\sigma_{max} = 1$ and $\xi_{max} = 10$). Injecting Eq.(2) and Eq.(3) into Eq.(1) gives:

$$TP_n^{i+1} = d_n P_n^i + b_n S_n^i \quad (4)$$

Where

$$a_n = \frac{i}{2nk_0}\frac{z_0}{a^2}\frac{\Delta\sigma}{\Delta\xi^2},$$
$$b_n = i\frac{\beta n k_0 z_0}{2c_0\rho_0}\Delta\sigma, \quad (5)$$
$$d_n = 1 - n^2\alpha_0 z_0\Delta\sigma,$$

$$P_n^{i+1} = \begin{pmatrix} p_n^{1,i+1} \\ \vdots \\ p_n^{J,i+1} \end{pmatrix}, \quad S_n^i = \begin{pmatrix} S_n^{1,i} \\ S_n^{2,i} \\ \vdots \\ S_n^{J,i} \end{pmatrix}$$

and $$s_n^{i,j} = \sum_{m=1}^{i-1} p_m^{i,j} p_{n-m}^{i,j} + 2\sum_{m=i+1}^{N} p_m^{i,j}\left(p_{m-n}^{i,j}\right)^*$$

N is the maximum number of harmonics considered in the integration, $(p_{m-n})^*$ is the conjugate complex of p_{m-n} and $\alpha = Dk_0^2/2c_0$ is the linear absorption coefficient of the medium.

The matrix T is:

$$T = \begin{pmatrix} 1-2a_n & a_n a_r & 0 & \cdots\cdots & 0 & 0 \\ a_n b_r & 1-2a_n & a_n a_r & \cdots\cdots & 0 & 0 \\ 0 & a_n b_r & 1-2a_n & \cdots\cdots & 0 & 0 \\ \vdots & \vdots & \vdots & & \vdots & \vdots \\ 0 & 0 & 0 & & 1-2a_n & a_n a_r \\ 0 & 0 & 0 & & a_n b_r & 1-2a_n \end{pmatrix} \quad (6)$$

$$a_r = \left(1 + \frac{\Delta\xi}{2\xi}\right) \quad b_r = \left(1 - \frac{\Delta\xi}{2\xi}\right) \quad (7)$$

Then the solution of Eq.(4) is

$$P_n^{i+1} = T^{-1}\left\{d_n P_n^i + b_n S_n^i\right\} \quad (8)$$

The inverse of T is calculated using the Thomas' algorithm (or LU method) [17].

Our algorithm is initialized by the source conditions bellow:

$$\begin{cases} p_n(\xi,0) = 0 & n \neq 1 \\ p_1(\xi,0) = p_0 f(\xi) & if \ |\xi| \leq 1 \\ p_1(\xi,0) = 0 & elsewhere \end{cases} \quad (9)$$

f(ξ) is a function that describes the spatial distribution at the source. In the present paper we consider three shapes:

- Uniform: $f(\xi) = 1$,
- Exponential: $f(\xi) = \exp\left(-B\xi^2\right)$,
- And Bessel: $f(\xi) = J_0\left(A\xi\right)$.

A, B are parameters that permits to modify the distribution shape. The figure 1 shows these distributions for A=2.4 and B=3. The value of A is chosen to maintain only the Bessel function's main lobe. And B's value permits to have a small power gap at $|\xi| = 1$ and also to maintain an exponential lobe sufficiently large.
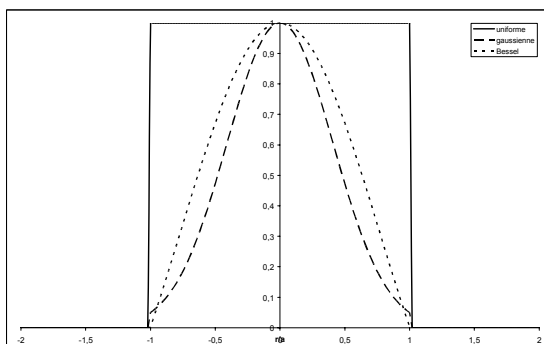

Fig.2 Power distributions at the source for uniform, exponential and Bessel beam sources

3   Algorithm validation

In order to validate our algorithm we compare the results with those obtained by the Bergen code. The figure 3 shows the axial distributions of the fundamental and the second harmonic respectively. The curves show a good agreement.
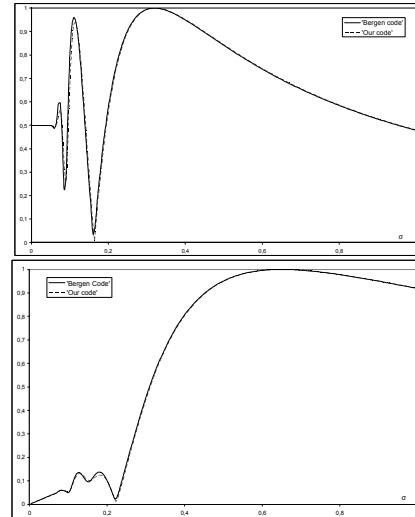

Fig.2 Axial distributions of fundamental (top) and second harmonic (down) obtained by our code (solid) and Bergen code (dotted)

4   Results and discussions

The figures 3, 4 and 5 present the axial distributions of fundamental and second harmonic for the uniform, exponential and Bessel beam source respectively. The magnitude is normalized with respect to the maximum and the curves are presented vs. σ.
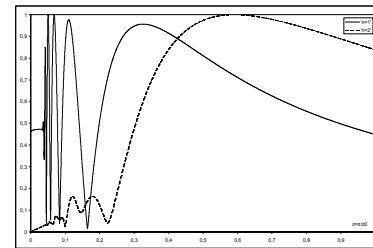

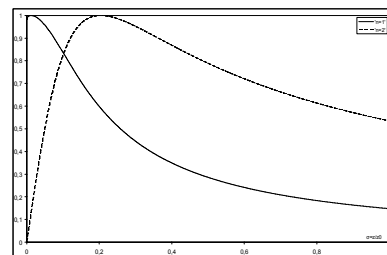Fig. 3 The fundamental (solid) and the second harmonic (dotted) for the uniform source

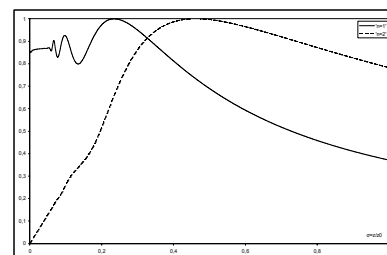Fig. 4 The fundamental (solid) and the second harmonic (dotted) for the exponential source

Fig. 5 The fundamental (solid) and the second harmonic (dotted) for the Bessel beam source

The exponential source (fig.4) shows no nearfield oscillations for both the fundamental and the second harmonic. The fundamental curve decreases from the source which is due to the diffraction effect and the energy transfer to the second and higher harmonics. The second harmonic maximum is close to the source. These results fit with the Gaussian beam propagation. Bessel source (fig.5) shows less amplitude oscillations in the nearfield zone. We can conclude here that the amplitude of the nearfield zone oscillations is related to the shaped of the source distribution.

At the other hand the last maxima for both the fundamental and the second harmonic move according to the shape of the source distribution. We had reported this when we studied the cosine shape source [6].

The figures 6 to 8 and 9 to 11 show the transverse distributions of the fundamental and the second harmonic respectively for the studied sources in the nearfield ($\sigma = 0.16$), at $\sigma = 0.33$, corresponding to the fundamental's last maximum for the uniform source's case, and the farfield ($\sigma = 0.65$). The magnitude is normalized with respect to the maximum and the curves are presented vs. ξ.

The sidelobes, for both fundamental and second harmonic, are presents only in the case of the source uniform. It can be explained by the fast transition at the edge of the source which causes oscillations in the lateral distributions of the field. These phenomena suggested that a lateral propagation occurs.

The exponential beam width increases from the source ($\sigma = 0$) showing that no focusing effects occur. However it can be shown that the fundamental (fig. 7) is larger than the second harmonic one (fig. 10). On the other side the Bessel beams are less diffractive since their widths are slightly changing with propagation (fig. 8 and 11).
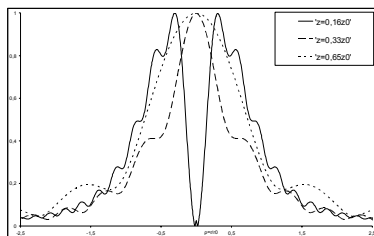

Fig.6 Lateral distributions of the uniform source's fundamental
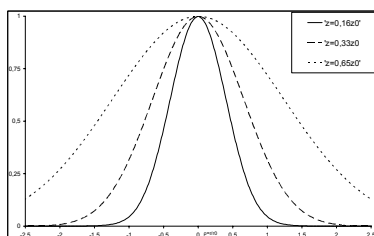

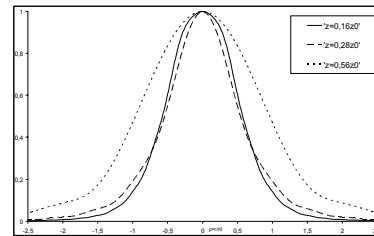Fig.7 Lateral distributions of the exponential source's fundamental

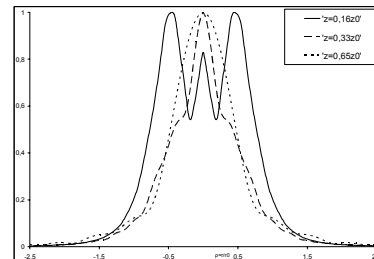Fig.8 Lateral distributions of the Bessel source's fundamental

Fig.9 Lateral distributions of the uniform source's second harmonic
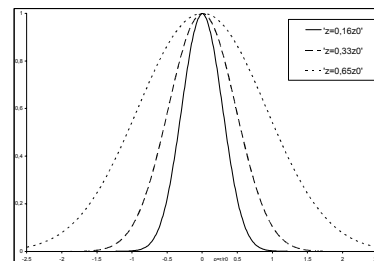

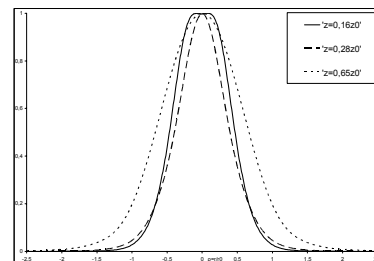Fig.10 Lateral distributions of the exponential source's second harmonic

Fig.11 Lateral distributions of the Bessel source's second harmonic

The second harmonic is narrower than the fundamental in all cases. Considering the lateral distributions of fig 6 to 11, the -3dB widths are given by the table 1. The values are calculated with respect to the source diameter.

At the farfield ($\sigma = 0.65$) the uniform aperture presents the smallest width. However in the nearfield ($\sigma = 0.16$) this source presents the largest width for both the fundamental and second harmonic. However for the exponential source the fundamental and second harmonic show the narrowest beam in the nearfield ($\sigma = 0.16$) and the largest beam at $\sigma \geq 0.33$.

The Bessel beams show, at $\sigma = 0.33$, a narrower width than at $\sigma = 0.16$ or $\sigma = 0.65$. Hence we note a focusing effect even for plane Bessel source. Further the second harmonic show a beam width that still under the limit of 50% of the source diameter. This could be a good index for using the Bessel sources in the imaging systems.

The figure 12 shows the radiation pattern of the fundamental in the (σ, ξ) plan for the studied apertures. The Bessel source's fundamental shows a quasi constant width and a reduced sidelobes throughout the region $\sigma \le 0.6$. In the exponential source case the

fundamental beam is clearly enlarging since $\sigma = 0.3$. The uniform source's fundamental present, in near field, a beam width almost constant but it shows high level sidelobes.

	Uniform			Bessel			Exponential		
σ	0.16	0.33	0.65	0.16	0.33	0.65	0.16	0.33	0.65
Fundamental (%)	66	26.5	53	44	37	69	33	50.5	103
Second harmonic (%)	66	17	34.5	38	27	48	24	40	76

Table 1: -3dB beam widths for the fundamental and the second harmonic of the studied sources' shapes
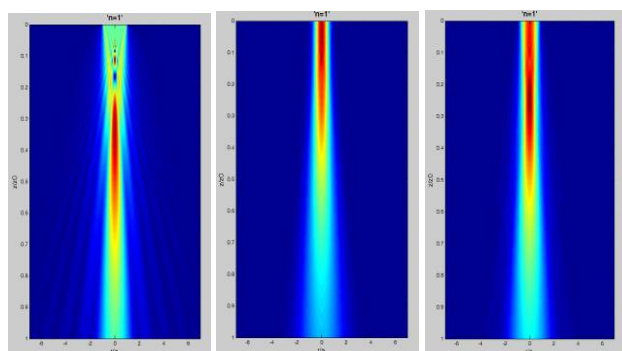

Fig. 12 Fundamental radiation patterns for uniform (left) exponential (medium) and Bessel (left) aperture

The figure 13 presents the spatial distributions of the second harmonic beams.

In the exponential source's case the second harmonic is generated earlier and enlarging with propagation distance. The Bessel source presents a narrower width in the transition zone ($0.3 \le \sigma \le 0.4$). Elsewhere the beam is slightly larger and shows attenuated sidelobes.
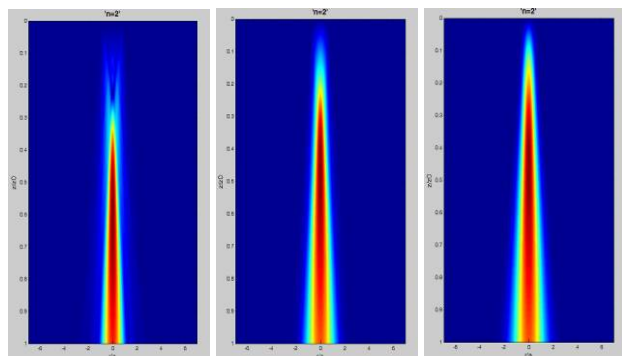

Fig. 13 Second harmonic radiation patterns for uniform (left) exponential (medium) and Bessel (left) aperture

5   Conclusion

In this paper we developed an integration algorithm for the KZK equation. The code is based on the spectral method and allows studying several sources' shapes. In order to

validate the code the results are compared to those obtained by Bergen code. We noticed a very good agreement.

Exponential and Bessel beams are the two source's shapes studied. The results obtained by each of them are compared to those of uniform aperture.

We concluded that we can choose a suitable distribution power on the source in order to minimize the level of the nearfield oscillations. We can also find a source shape leading to harmonic beam with less diffraction and attenuated sidelobes

We noted that the studied Bessel source (A=2.4) presents, in the nearfield and the transition zone, a quasi constant beam width and attenuated sidelobes. This could favour this source vs. the exponential one whose beams are enlarging with propagation.

The Bessel shape source's features can be interesting for the medical imaging fields. Furthermore the production of a Bessel beam is difficult using a monodimensional PZT transducer. Yet the recent progress concerning the micromachined transducers [18] makes it possible to generate complex power distributions especially Bessel beams.

Acknowledgement

References

[1] K. K. SHUNG; Ultrasonic transducers and array in diagnostic ultrasound imaging and blood flow measurements; Ed. Taylor & Francis Group 2006.

[2] G. S. KINO; *Wave Propagation with finite exciting sources* in *Acoustic waves: device, imaging and analogue signal processing* Ed. Rentice-Hall, Inc. 2000.

[3] T.G. MUIR, *Nonlinear effects in acoustic imaging*; Acoust. Imag. Vol. 9 No. 93; 1980.

[4] V. F. HUMPHREY; *Nonlinear propagation in ultrasonic fields: measurements, modelling and harmonic imaging*; Ultrason. 38; 2000; pp 267-72.

[5] D. KOURTICHE, L. AIT ALI, A. CHITNALAH, M. NADI; *Theoretical study of harmonic generation sound beams in case of uniform, exponential and cosinusoidal apertures*; 2001 Proceeding Of the 23rd Annual EMBS International Conference, October 25-28, Istanbul, Turkey.

[6] H. JAKJOUD, A. CHITNALAH, N. AOUZALE, D. KOURTICHE; *Study of the effect of an ultrasonic source's shape on the generated harmonics*; International Conference on Approximation Methods and Numerical Modelling in Environment and Natural Resources; Granda, Spain July 11-13, 2007 (MAMERN'07); pp. 137-42.

[7] J. DURNIN, *Exact solution for nondiffracting beams. I. The scalar theory*; OPT. Soc. Am. Vol. 4, No. 4; April 1987; pp 651-54.

[8] D. DING, Z. LU; *The second harmonic component in the Bessel beam*; Appl. Phys. Lett. ; Vol. 68 No. 608; Novem. 1995; pp 608-10.

[9] H. JAKJOUD "Etude de la possibilité de caractérisation des matériaux par la mesure du paramètre de non linéarité ultrasonore " ; Master thesis, University CADI AYYAD, 2005.

[10] E.A. ZABOLOTSKAYA, R.V. KHOKHLOV; *Quasi-plane waves in the nonlinear acoustics of confined beams*; Soviet Physics-Acoustics; Vol.15; n°1; July-Sept. 1969.

[11] V.P. KUZNETSOV; *Equations of nonlinear acoustics*; Soviet Physics-Acoustics; Vol.16; n° 4; April-June 1971.

[12] S.I. AANNOSEN, T. BARKVE, J.N. TJOTTA, S. TOJOTTA; *Distortion and harmonic generation in the nearfield of a finite amplitude sound beam*; J. Acoust. Soc. Am. 75 (3); March 1983.

[13] J. BERNTSEN; *Numerical calculations of finite amplitude sound beams*; Font. Of Nonlinear Acous. Proc. Of 12 th ISNA edit. M.F.HAMILTON, T.BLACKSTOCK; Elsevier Science Publishers LTD; London 1990.

[14] M.F. HAMILTON, J.N. TJOTTA, S. TJOTTA; *Nonlinear effects in the farfield of a directive sound source*; J. Acoust. Soc. Am 78 (1) July 1985.

[15] A.C. BAKER, K. ANASTASIADIS, V.F. HUMPHREY; *The nonlinear pressure field of a plane circular piston: Theory and Experiment*; J. Acoust. Soc. Am 84(4) Oct. 1988.

[16] S. NACHEF, D. CATHIGNOL, J. N. TJØTTA, A. M. BERG, S. TJØTTA ; *Investigation of a high intensity sound beam from a plane transducer. Experimental and theoretical results*; .J. Acoust. Soc. Am 98 (4); 1995.

[17] J. P. NOUGIER; *Méthodes de calcul numérique*; 2e édition ; Masson 1985 pp 38-41.

[18] S. A. ANBALAGAN, G. UMA, M. UMAPATHY; *Modeling and Simulation of Capacitive Micromachined Ultrasonic Transducer (CMUT)*; J. Phy. Conf. Series 34 (2006) pp 595-600; Intern. MEM Conf. 2006.